Self-Organizing and Stochastic Behaviors During the Regeneration of Hair Stem Cells

Maksim V. Plikus, *et al.*

Science **332**, 586 (2011);
DOI: 10.1126/science.1201647

8. P. G. D. Feulner, F. Kirschbaum, V. Mamonekene, V. Ketmaier, R. Tiedemann, *J. Evol. Biol.* **20**, 403 (2007).
9. C. D. Hopkins, *Am. Zool.* **21**, 211 (1981).
10. M. A. Xu-Friedman, C. D. Hopkins, *J. Exp. Biol.* **202**, 1311 (1999).
11. B. A. Carlson, in *Communication in Fishes*, F. Ladich, S. P. Collin, P. Moller, B. G. Kapoor, Eds. (Science Publishers, Enfield, NH, 2006), vol. 2, pp. 805–848.
12. C. C. Bell, T. Szabo, in *Electroreception*, T. H. Bullock, W. Heiligenberg, Eds. (John Wiley & Sons, New York, 1986), pp. 375-421.
13. C. D. Hopkins, A. H. Bass, *Science* **212**, 85 (1981).
14. P. G. D. Feulner, M. Plath, J. Engelmann, F. Kirschbaum, R. Tiedemann, *Biol. Lett.* **5**, 225 (2009).
15. P. Machnik, B. Kramer, *J. Exp. Biol.* **211**, 1969 (2008).
16. M. E. Arnegard, B. S. Jackson, C. D. Hopkins, *J. Exp. Biol.* **209**, 2182 (2006).
17. A. H. Bass, in *Electroreception*, T. H. Bullock, W. Heiligenberg, Eds. (Wiley, New York, 1986), pp. 13–70.
18. H. H. Zakon, in *Electroreception*, T. H. Bullock, W. Heiligenberg, Eds. (Wiley, New York, 1986), pp. 103–156.
19. A. H. Bass, C. D. Hopkins, *J. Morphol.* **174**, 313 (1982).
20. W. Harder, *Z. Vgl. Physiol.* **59**, 272 (1968).
21. S. Lavoué, C. D. Hopkins, A. K. Toham, *Zoosystema* **26**, 511 (2004).
22. N. Post, G. von der Emde, *Physiol. Behav.* **68**, 115 (1999).
23. P. Moller, J. Serrier, D. Bowling, *Ethology* **82**, 177 (1989).
24. B. C. O'Meara, C. Ané, M. J. Sanderson, P. C. Wainwright, *Evolution* **60**, 922 (2006).
25. D. L. Rabosky, S. C. Donnellan, A. L. Talaba, I. J. Lovette, *Proc. Biol. Sci.* **274**, 2915 (2007).
26. M. J. Ryan, *Proc. Natl. Acad. Sci. U.S.A.* **83**, 1379 (1986).
27. O. Seehausen *et al.*, *Nature* **455**, 620 (2008).
28. Y. Terai *et al.*, *PLoS Biol.* **4**, e433 (2006).
29. J. B. Sylvester *et al.*, *Proc. Natl. Acad. Sci. U.S.A.* **107**, 9718 (2010).
30. C. A. Shumway, *Brain Behav. Evol.* **72**, 123 (2008).

Acknowledgments: We thank C. D. Hopkins and J. R. Gallant for help with field work, J. P. Friel (Cornell University Museum of Vertebrates) for providing specimens, and S. Lavoué and J. P. Sullivan for providing *cytb* sequences (GenBank accession numbers provided in table S1). Supported by NSF IOS-0818390 (B.A.C.); L.J.H. was supported by NSF DEB-0919499.

Supporting Online Material

www.sciencemag.org/cgi/content/full/332/6029/583/DC1
Materials and Methods
Figs. S1 to S6
Tables S1 to S3
References

10 December 2010; accepted 21 March 2011
10.1126/science.1201524

Self-Organizing and Stochastic Behaviors During the Regeneration of Hair Stem Cells

Maksim V. Plikus,[1] Ruth E. Baker,[2] Chih-Chiang Chen,[1,3] Clyde Fare,[4] Damon de la Cruz,[1] Thomas Andl,[5] Philip K. Maini,[2,6] Sarah E. Millar,[7] Randall Widelitz,[1] Cheng-Ming Chuong[1,8]*

Stem cells cycle through active and quiescent states. Large populations of stem cells in an organ may cycle randomly or in a coordinated manner. Although stem cell cycling within single hair follicles has been studied, less is known about regenerative behavior in a hair follicle population. By combining predictive mathematical modeling with in vivo studies in mice and rabbits, we show that a follicle progresses through cycling stages by continuous integration of inputs from intrinsic follicular and extrinsic environmental signals based on universal patterning principles. Signaling from the WNT/bone morphogenetic protein activator/inhibitor pair is coopted to mediate interactions among follicles in the population. This regenerative strategy is robust and versatile because relative activator/inhibitor strengths can be modulated easily, adapting the organism to different physiological and evolutionary needs.

Continuous stem cell (SC) regeneration is essential for the maintenance of many adult organs, for example, in the bone marrow, skin, and gastrointestinal tract. Although regenerative behavior within a single SC cluster such as the hair bulge (*1*) or intestinal villi (*2*) has been studied, it is largely unknown how the regenerative behavior in populations of these SC clusters is coordinated. During development, thousands of cells can self-organize into anatomic structures and patterns by coordinating just a few morphogenetic signals (*3*), as seen in the periodic patterning of skin appendages (*4*, *5*). We hypothesize that the regenerative cycling of adult organ SCs can be similarly coordinated by diffusible signals and self-organize into spatiotemporal regenerative patterns.

Hair offers a suitable experimental model because hair follicles (HFs) cycle through phases of growth (anagen) and rest (telogen) (*6*). SCs are clustered in hair bulges, making them easier to study than SCs in other organs, where they are usually scattered randomly (*7*) (fig. S1A). Growing hairs produce pigmentation patterns that allow simultaneous monitoring of the regenerative behavior of thousands of SCs (Fig. 1A) (*8*, *9*). Additionally, the skin is flat, restricting interactions between HFs to two dimensions, further simplifying the analysis.

We developed a cellular automaton (CA) model consisting of a regular grid of automata, with one automaton representing one HF (fig. S1B) (*10*). The eight automata surrounding one automaton are defined as its neighbors. With time, the state of each automaton changes according to rules that take into account the state of neighboring automata. Automata in certain states can interact, generating complex, self-organizing patterns based on a simple set of rules. Such patterning behavior can be globally modulated by simple rule changes in local automaton-to-automaton interactions (*11*).

To form regenerative patterns, activating signals among SCs should be able to spread and stop. This is possible when SCs can differentially respond to the same signal at different times of their regenerative cycle. We previously identified four functional phases in the hair regenerative cycle: signal-propagating (P) and nonpropagating phases (A), and phases refractory (R) and competent (C) to such signals (*12*). Telogen HFs in R phase cannot enter anagen because bone morphogenetic proteins (BMPs) in the surrounding skin macroenvironment keep hair SCs quiescent (*12*). Telogen HFs in C phase are devoid of these inhibitors and can enter anagen as long as the sum of intrinsic and extrinsic activators is above the threshold. Intrinsic activators are produced as the result of hair SCs and dermal papilla interactions. Extrinsic activators come from neighboring P-phase anagen HFs and represent a form of collective positive feedback. Thus, HFs can enter anagen in two ways: autonomously, depending on the level of intrinsic activation, or nonautonomously, when activators are delivered by the surrounding macroenvironment. The probability of anagen entry is based on the sum of these fluctuating inputs.

We used mathematical simulations to test the sufficiency and robustness of this model. We show that the CA model encompassing P→A→R→C cycling can reproduce the full spectrum of hair regenerative patterns observed in mice: formation of initiation centers, wave spreading, maintenance of borders, and border instability (Fig. 1B, fig. S2, and table S1).

For a model to be robust and capture conserved patterning principles, it should be capable of explaining the diverse regenerative patterns seen in mutant mice and other animals. The duration of each phase of the regenerative cycle depends on the relative strengths of activators and inhibitors (Fig. 1A). We suggest that dif-

[1]Department of Pathology, University of Southern California (USC), Los Angeles, CA 90033, USA. [2]Centre for Mathematical Biology, Mathematical Institute, 24-29 St. Giles', Oxford OX1 3LB, UK. [3]Institute of Clinical Medicine and Department of Dermatology, National Yang-Ming University and Department of Dermatology, Taipei Veterans General Hospital, Taipei, Taiwan. [4]Life Sciences Interface Doctoral Training Centre, Wolfson Building, Parks Road, Oxford OX1 3QD, UK. [5]Vanderbilt University Medical Center, Nashville, TN 37232, USA. [6]Oxford Centre for Integrative Systems Biology, Department of Biochemistry, South Parks Road, Oxford OX1 3QU, UK. [7]Department of Dermatology, University of Pennsylvania, Philadelphia, PA 19104, USA. [8]Research Center for Developmental Biology and Regenerative Medicine, National Taiwan University, Taiwan.

*To whom correspondence should be addressed. E-mail: cmchuong@usc.edu

fusible signaling molecules used for regulating SC activities within the HF are coopted to mediate interactions between neighboring HFs. Activator-driven propagation of regenerative waves and inhibitor-driven halting of wave propagation can be potentiated by respective ligands or dampened by antagonists secreted between HFs by the skin macroenvironment. Together, HF and skin macroenvironment–derived ligands and antagonists should combine to produce unique signaling profiles that define properties of P→A→R→C phases (fig. S3). We assigned generic signaling profiles for each of the four phases in terms of the activator/inhibitor ratio: for P, high/low; A, high/high; R, low/high; and C, low/low (Fig. 1A). We undertook predictive modeling by using our CA framework to anticipate how regenerative patterns might be altered by changing the level of hypothetical activators or inhibitors (Fig. 1B, fig. S3, and table S1). The key prediction from this model is that the strength of SC coupling can be weakened by either inhibitory pathway ligands or activating pathway antagonists.

Indeed, previously we showed that inhibitory BMP pathway ligands produced by the skin macroenvironment maintain telogen HFs in R phase and prevent them from being activated by the advancing regenerative wave (*12*). To identify activating pathway(s) involved in SC coupling, we began by matching expression patterns of various diffusible antagonists with the signature pattern predicted by the CA model: P, low; A, high; R, high; and C, low. *Dkk1* and *Sfrp4*, both diffusible WNT pathway antagonists, prominently fit this expression pattern (Fig. 2B and fig. S5). Simultaneously, multiple WNT ligands are expressed by anagen HFs (fig. S5B) (*13*) and, in principle, can serve as diffusible activators to mediate regenerative coupling between HFs. This scenario predicts that competing WNT ligands and antagonists produce distinct patterns of WNT signaling: WNT is activated in C-phase telogen HFs adjacent to P-phase anagen HFs but not in the same C-phase HFs next to A-phase anagen HFs.

To gauge WNT signaling, we used *BAT-gal* and *cond-lacZ* WNT reporter mice, where lacZ expression marks canonical WNT pathway activation. Indeed, WNT reporter mice show these predictions to be true. Massive WNT pathway activation is seen in C-phase HFs ahead of the P→C regenerative wave front (fig. S8, I and K) but not along the A-C border (fig. S8L). According to CA model predictions, the activating pathway should demonstrate stochastic signaling in C- but not R-phase HFs, forming the basis for rare spontaneous C→P activation events. We found striking differences in WNT signaling between R and C phases. Although there is almost no WNT activation in R phase, both reporter mice show many stochastically distributed WNT-active telogen HFs in C phase (Fig. 2E and fig. S8). The majority of WNT-active HFs are solitary (4.9% in *BAT-gal* and 5% in *cond-lacZ*), but groups of two to four WNT-active HFs are very rare (0.23 to 0.01%) (table S3). This WNT activity is localized not to SCs but to adjacent dermal papillae (DPs) (fig. S8C). We found that 99.9% of all spontaneous WNT activation events in DPs do not translate into spontaneous anagen initiations. However, when WNT activation occurs in groups of five or more DPs simultaneously (<0.01%), it leads to new anagen activation (fig. S8J). This illustrates the stochastic nature of activation events predicted by the model and implies that HFs work synergistically toward successful anagen reentry.

We tested the functional role of WNT signaling locally with protein-coated beads and globally with transgenic mice. Local injection of Wnt3a beads induces new regenerative waves, whereas injection of Dkk1 beads disrupts advancement of the existing regenerative wave (Fig. 2, C and D, and fig. S7). Furthermore, when Wnt7a is overexpressed in *K14-Wnt7a* mice, there is shortening of R phase (from 28 to 12 days) and enhanced SC activation, evidenced by many more spontaneous anagen initiation events and faster wave spreading compared with that seen in WT (Fig. 2A and figs. S6 and S10, B and C). In *cond-lacZ;K14-Wnt7a* mice, nearly 100% of DPs become WNT-active in C and even R phases (Fig. 2F and fig. S8, G and H), but no anagen reentry is observed in early R phase. A simultaneous decrease in inhibitory BMP signaling upon an R→C transition is essential for WNT-mediated anagen reentry.

By fulfilling multiple CA model predictions for a hypothetical activator, WNT signaling emerges as the key pathway for mediating regenerative coupling between hair SCs. Our data show that successful anagen reentry requires both down-regulation of BMP in the macroenvironment and spontaneous up-regulation of WNT activity in DPs (fig. S8M). (i) Loss of inhibitors (BMP ligands and WNT antagonists) from the skin macroenvironment in C phase enables HFs to express fluctuating spontaneous WNT activity in DPs. (ii) Such WNT activity in a single HF is

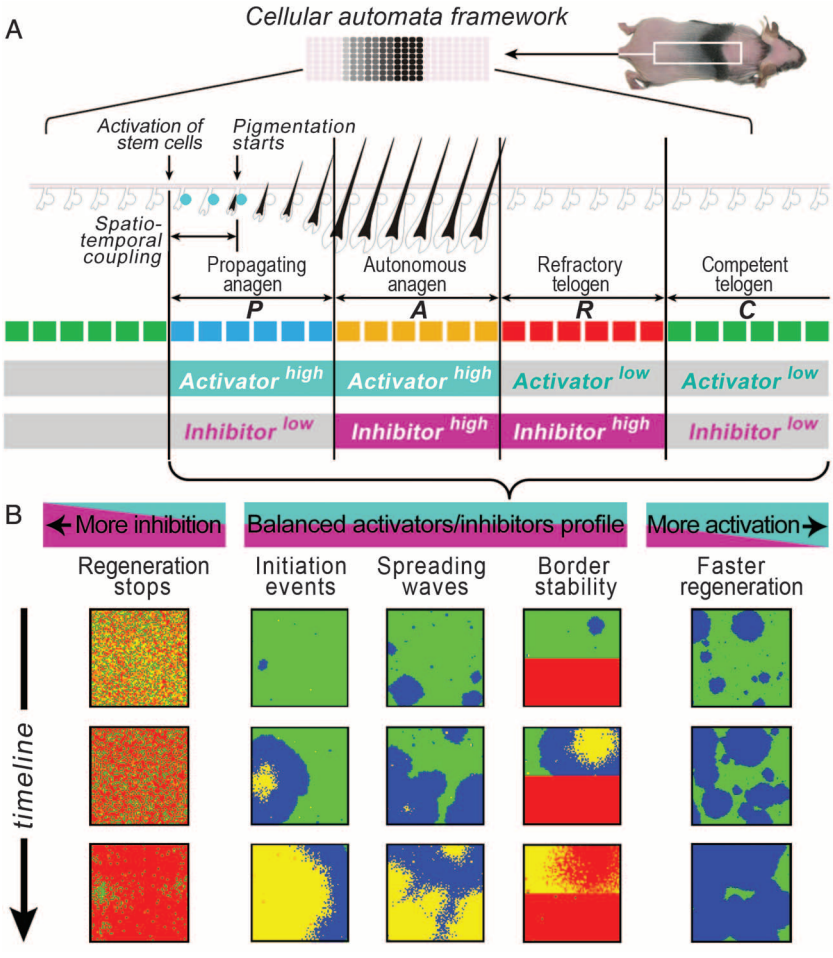

Fig. 1. A two-dimensional CA model can predict regenerative patterns in a large population of hair SCs. (**A**) Skin pigmentation patterns result from color changes of many HFs when they collectively cycle through four phases: P (blue)→A (yellow)→R (red)→C (green). Distinct hypothetical activator/inhibitor signaling profiles can be assigned to all four phases. (**B**) A two-dimensional CA model, in which each color-coded element (automaton) represents a single HF (fig. S1B), can reproduce regenerative patterns observed in mice: spontaneous initiation, spreading waves, and stability of borders. The model can also predict changes in patterns when there are either more inhibitors or more activators.

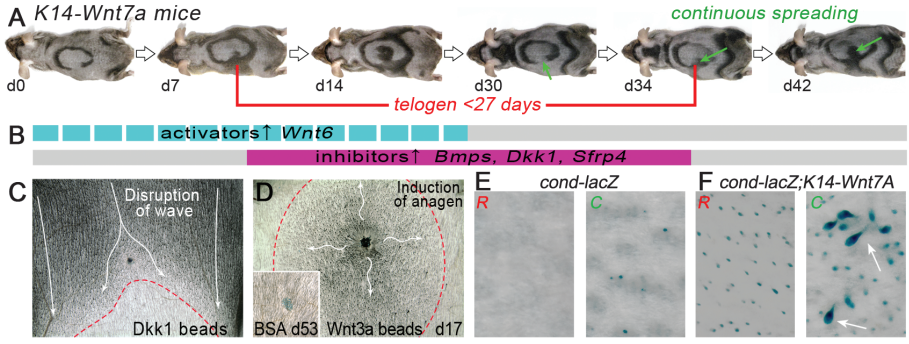

Fig. 2. WNT signaling plays an activating role in the coordinated regeneration of hair SCs in a follicle population. (**A**) Wnt7a overexpression in *K14-Wnt7a* mice results in regenerative patterns with shortened R phase, multiple spontaneous initiation centers, fast wave spreading, and lack of border stabilization (figs. S6 and S10). (**B**) Differential expression of key activators and inhibitors in the skin macroenvironment (data in fig. S5). (**C** and **D**) In bead implantation experiments, Wnt3a induces a new regenerative wave (D), whereas Dkk1 disrupts spreading of the existing regenerative wave (C) and control bovine serum albumin (BSA) has no effect (D, inset) (fig. S7). White arrows show directions of anagen spreading waves; red outlines mark anagen-telogen boundaries. (**E** and **F**) In *cond-lacZ* WNT reporter mice, spontaneous WNT activity (blue dots) occurs in DPs in C-phase but not R-phase telogen HFs. Large clusters of WNT-active DPs are very rare (table S3). In *cond-lacZ;K14-Wnt7a* mice, 100% of DPs become WNT-active throughout telogen, which induces many new anagen initiation events (white arrows) during C phase (fig. S8).

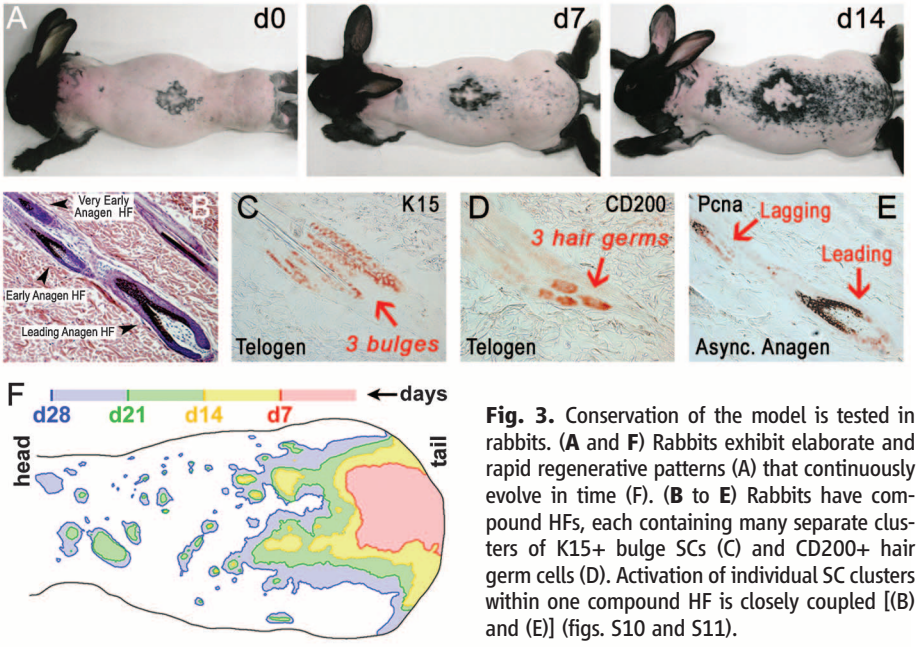

Fig. 3. Conservation of the model is tested in rabbits. (**A** and **F**) Rabbits exhibit elaborate and rapid regenerative patterns (A) that continuously evolve in time (F). (**B** to **E**) Rabbits have compound HFs, each containing many separate clusters of K15+ bulge SCs (C) and CD200+ hair germ cells (D). Activation of individual SC clusters within one compound HF is closely coupled [(B) and (E)] (figs. S10 and S11).

Fig. 4. A unifying model of coordinated regeneration of hair SCs. The CA model predicts how simple changes in the relative levels of activators and inhibitors change SC coupling efficiency and modulate duration of P→A→R→C phases (colors are based on Fig. 1A). This produces versatile hair regenerative patterns that help animals adapt to different physiological conditions. See fig. S16.

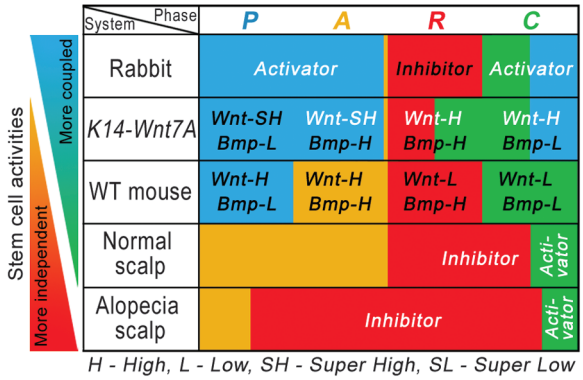

not sufficient to drive anagen reentry. When several DPs adopt a WNT-active status simultaneously, they reenforce each other, and C→P activation occurs stochastically. Indeed, WNT signaling in DPs was recently shown to be critical for their anagen-inducing effect, likely mediated by secondary FGF signaling (*14*). Alternatively, in regenerative waves the wave front carries many activators that induce all C-phase HFs to enter anagen.

Compared with mice, rabbits have more robust hair growth. They have compound HFs (fig. S12) (*15*), each containing multiple tightly packed SC clusters and DPs (Fig. 3, B to E, and fig. S11). The skin surface area of rabbits is also 30 times larger than in mice. We wanted to examine regenerative patterns in rabbits and see how our CA model fares against experimental data. We observed that C→P activations in all SC clusters within one compound HF are closely coupled, and in the context of our CA model they behave as one "supercluster" (one automaton) of SCs. Rabbits display complex, fractal-like regenerative patterns (Fig. 3, A and F, and figs. S9 and S10) closely reminiscent of patterns generated by our model (fig. S4A). By exploring their fractal geometry, we show that large pieces of regenerative patterns in rabbits remain geometrically similar to much smaller pieces of themselves (fig. S14). Thus, the same CA principles are effective in managing regeneration of hair SCs regardless of their total number, arrangement, or organ size. Notably, pattern-forming signaling cues are likely conserved between mice and rabbits, because activation events readily spread from rabbit to mouse HFs in the cross-species grafting system, resulting in hybrid patterns (fig. S13).

Our modeling predicts that substantial increases in inhibiting signals or decreases in activating signals would reduce and eventually prevent coupling among HFs (Figs. 1B and 4). We see this in humans, where regenerative waves are observed in fetal scalp during the first two cycles (*16*) but disappear in the adult, when all HFs cycle independently and randomly (*17*). In adults, the lack of SC coupling makes hair regeneration depend solely on intrinsic activation mechanisms, making it particularly vulnerable to any decreases in intrinsic SC activation. Without coupling, such decreases can ultimately lead to baldness as seen in androgenic alopecia and "short anagen syndrome" (figs. S15 and S16A) (*18*).

We have shown how organ-wide SC management can be achieved. We speculate that during evolution integration of signals from single to multiple HFs across skin likely facilitated the formation of new mechanisms of regeneration. SC clusters can now be regulated as one entity, allowing organ regeneration to occur episodically with an intrinsic rate (fig. S16B, *y* axis). Cooption of key WNT and BMP signaling pathways from HFs by the skin macroenvironment allows for coupling between the SC clusters (fig. S16B, *x* axis). We conjecture that such a mechanism provides animals with a simple, yet robust and effective, way to coordinate the regeneration of very large SC pop-

ulations, which would otherwise be impossible with an intrinsic activation mechanism alone. We observe that regenerative hair patterns can differ in the same animal under different physiological conditions, allowing organisms to adapt to the environment (e.g., pregnancy in mice) (*12*). At the evolutionary scale, macroenvironmental regulation makes hair growth a trait that has high modulability. Lastly, beyond HFs, the experimental accessibility of this system offers a model for analyzing the fundamental principles of self-organizing behaviors in biological systems composed of coupled cycling elements.

References and Notes

1. E. Fuchs, *Cell Stem Cell* **4**, 499 (2009).
2. L. Li, H. Clevers, *Science* **327**, 542 (2010).
3. C.-M. Chuong, M. K. Richardson, *Int. J. Dev. Biol.* **53**, 653 (2009).
4. T. X. Jiang, H. S. Jung, R. B. Widelitz, C. M. Chuong, *Development* **126**, 4997 (1999).
5. S. Sick, S. Reinker, J. Timmer, T. Schlake, *Science* **314**, 1447 (2006); 10.1126/science.1130088.
6. K. S. Stenn, R. Paus, *Physiol. Rev.* **81**, 449 (2001).
7. R. J. Morris *et al.*, *Nat. Biotechnol.* **22**, 411 (2004).
8. N. Suzuki, M. Hirata, S. Kondo, *Proc. Natl. Acad. Sci. U.S.A.* **100**, 9680 (2003).
9. M. V. Plikus, C.-M. Chuong, *J. Invest. Dermatol.* **128**, 1071 (2008).
10. Materials and methods are available as supporting material on *Science* Online.
11. S. Wolfram, *A New Kind of Science* (Wolfram Media, Champaign, IL, 2002).
12. M. V. Plikus *et al.*, *Nature* **451**, 340 (2008).
13. S. Reddy *et al.*, *Mech. Dev.* **107**, 69 (2001).
14. D. Enshell-Seijffers, C. Lindon, M. Kashiwagi, B. A. Morgan, *Dev. Cell* **18**, 633 (2010).
15. H. J. Whiteley, *Nature* **181**, 850 (1958).
16. M. Cutrone, R. Grimalt, *Eur. J. Pediatr.* **164**, 630 (2005).
17. J. Halloy, B. A. Bernard, G. Loussouarn, A. Goldbeter, *Proc. Natl. Acad. Sci. U.S.A.* **97**, 8328 (2000).
18. R. J. Antaya, E. Sideridou, E. A. Olsen, *J. Am. Acad. Dermatol.* **53** (suppl. 1), S130 (2005).

Acknowledgments: C.-M.C. is supported by National Institute of Arthritis and Musculoskeletal and Skin Diseases RO1-AR42177, AR60306, and AR47364; S.E.M. by RO1-AR47709; R.E.B. by a UK Engineering and Physical Sciences Research Council First grant; P.K.M. by a Royal Society Wolfson Research Merit Award; and M.V.P. by a California Institute for Regenerative Medicine postdoctoral grant. There is a USC patent application partially based on the work in this study on the compositions and methods to modulate hair growth.

Supporting Online Material

www.sciencemag.org/cgi/content/full/332/6029/586/DC1
Materials and Methods
Figs. S1 to S16
Tables S1 to S3
Movies S1 to S9

14 December 2010; accepted 25 March 2011
10.1126/science.1201647

Conserved Eukaryotic Fusogens Can Fuse Viral Envelopes to Cells

Ori Avinoam,[1] Karen Fridman,[1] Clari Valansi,[1] Inbal Abutbul,[2] Tzviya Zeev-Ben-Mordehai,[3] Ulrike E. Maurer,[4] Amir Sapir,[1]* Dganit Danino,[2] Kay Grünewald,[3,4] Judith M. White,[5] Benjamin Podbilewicz[1]†

Caenorhabditis elegans proteins AFF-1 and EFF-1 [*C. elegans* fusion family (CeFF) proteins] are essential for developmental cell-to-cell fusion and can merge insect cells. To study the structure and function of AFF-1, we constructed vesicular stomatitis virus (VSV) displaying AFF-1 on the viral envelope, substituting the native fusogen VSV glycoprotein. Electron microscopy and tomography revealed that AFF-1 formed distinct supercomplexes resembling pentameric and hexameric "flowers" on pseudoviruses. Viruses carrying AFF-1 infected mammalian cells only when CeFFs were on the target cell surface. Furthermore, we identified fusion family (FF) proteins within and beyond nematodes, and divergent members from the human parasitic nematode *Trichinella spiralis* and the chordate *Branchiostoma floridae* could also fuse mammalian cells. Thus, FF proteins are part of an ancient family of cellular fusogens that can promote fusion when expressed on a viral particle.

Membrane fusion is critical for many biological processes such as fertilization, development, intracellular trafficking, and viral infection (*1*–*6*). Current models of the molecular mechanisms of membrane fusion rely on experimental and biophysical analyses performed on viral and intracellular, minimal, fusion-mediating machineries. Yet, how well these models correspond to the mechanisms of cell-cell fusion is unknown (*4*, *5*). *Caenorhabditis elegans* fusion family (CeFF) proteins were identified as *C. elegans* fusogens that are expressed at the time and place of cell fusion in vivo (*7*, *8*). Expression of CeFF proteins is essential for developmental cell fusion via hemifusion and sufficient to fuse cells in vivo and in insect cell cultures (*8*–*10*).

To identify putative fusion family (FF) members in other species, we conducted sequence comparisons (*4*, *11*). These comparisons yielded putative members in 35 nematodes, two arthropods (*Calanus finmarchicus* and *Lepeophtheirus salmonis*), a ctenophore (*Pleurobrachia pileus*), a chordate (*Branchiostoma floridae*), and a protist (*Naegleria gruberi*) (Fig. 1A). FF proteins are putative members of the "mostly β sheet super family" and share a pattern of cysteines, implying that they are conserved at the level of structure (fig. S1).

To determine whether divergent FF proteins maintained their function as fusogens through evolution, we expressed FF proteins from the human parasitic nematode *Trichinella spiralis (Tsp-ff-1)* and the chordate *B. floridae* (*Bfl-ff-1*) in baby hamster kidney (BHK) cells and compared their fusogenic activity to AFF-1 (Fig. 1, B to F). These orthologs share 26 and 22% sequence identity with AFF-1, respectively. We observed, by immunofluorescence, 28 ± 4% and 37 ± 7% multinucleation in cells transfected with *Tsp-ff-1* and *Bfl-ff-1*, compared with 26 ± 2% and 4 ± 3% multinucleation in controls transfected with *aff-1* and empty vector, respectively (Fig. 1F) (*11*). In addition, when we expressed the EFF-1 paralog from the nematode *Pristionchus pacificus* in *C. elegans* embryos, we detected ectopic fusion of cells that normally do not fuse (fig. S2). Thus, FF proteins represent a conserved family of cellular fusogens.

To explore whether FF proteins can functionally substitute for viral fusogens, we complemented VSVΔG pseudoviruses with AFF-1 (Fig. 2 and fig. S3). We initially used a recombinant vesicular stomatitis virus (VSV) called VSVΔG, in which the glycoprotein G (VSVG) gene was replaced by a green fluorescent protein (GFP) reporter, to infect BHK cells overexpressing VSVG (*11*–*16*). The resulting VSVΔG-G viruses were capable of only a single round of infection, manifested by the production of GFP. We achieved complementation with AFF-1 by VSVΔG-G infection of BHK cells expressing AFF-1 (BHK–AFF-1), which generated pseudotyped particles carrying the nematode fusogen (VSVΔG–AFF-1). We biochemically validated incorporation of AFF-1 into VSVΔG pseudotypes by SDS–polyacrylamide gel electrophoresis, Coomassie staining, silver staining, immunoblotting, and mass spectrometry (*11*). We found that the major proteins on VSVΔG–AFF-1 were the viral proteins N, P, L, M, and AFF-1. For comparison, we also analyzed VSVΔG-G and VSVΔG (fig. S4 and table S5). Infection of BHK–AFF-1 cells with VSVΔG–AFF-1 showed a 600-fold increase compared with infection of BHK control cells not expressing AFF-1 (Fig. 2A). Although infection due to residual VSVG-complemented VSVΔG (VSVΔG-G) was negli-

[1]Department of Biology, Technion–Israel Institute of Technology, Haifa 32000, Israel. [2]Department of Biotechnology and Food Engineering and The Russell Berrie Nanotechnology Institute, Technion–Israel Institute of Technology, Haifa 32000, Israel. [3]Oxford Particle Imaging Centre, Division of Structural Biology, Wellcome Trust Centre for Human Genetics, University of Oxford, Oxford, OX3 7BN, UK. [4]Department of Molecular Structural Biology, Max-Planck Institute of Biochemistry, D-82152 Martinsried, Germany. [5]Department of Cell Biology, University of Virginia, Charlottesville, VA 22908, USA.

*Present address: Howard Hughes Medical Institute and Division of Biology, California Institute of Technology, Pasadena, CA 91125, USA.

†To whom correspondence should be addressed. E-mail: podbilew@technion.ac.il